Analytical Solutions for One-dimensional Steady State Flow in Layered, Heterogeneous Unsaturated Soils under Uncertainties

Zhiming Lu[1], Dongxiao Zhang[2], and Bruce Robinson[1]

[1]Hydrology, Geochemistry, and Geology Group (EES-6)
MS T003, Los Alamos National Laboratory
Los Alamos, NM 87545

[2]Mewbourne School of Petroleum and Geological Engineering
University of Oklahoma, 100 East Boyd, SEC T301
Norman, OK 73019

For Submission to *Water Resources Research*

March 2, 2005

Abstract

In this study, we derive first-order analytical solutions to the pressure head moments (mean and variance) for one-dimensional steady state unsaturated flow in randomly heterogeneous layered soil columns under various random boundary conditions. We assume that the constitutive relation between the unsaturated hydraulic conductivity and the pressure head follows an exponential model, and treat the saturated hydraulic conductivity K_s as a random function and the pore size distribution parameter α as a random constant. The solution to the pressure head variance is an explicit function of the input variabilities. In addition, we also give solutions for the mean and variance of the unsaturated hydraulic conductivity. The first-order analytical solutions are compared with those from Monte Carlo simulations. These comparisons show that the analytical solutions are valid for relatively large variabilities of soil properties. We also investigate the effect of uncertain boundary conditions and the relative contribution of input variabilities to the head variance.

INDEX TERMS: 1805 Hydrology: Computational hydrology; 1849 Hydrology: Numerical approximation and analysis; 1869 Hydrology: Stochastic hydrology; 1873 Hydrology: Uncertainty assessment; 1875 Hydrology: Vadose zone; *KEYWORDS:* stochastic processes, unsaturated flow, heterogeneity, uncertainty quantification, analytical solutions

1 Introduction

Various analytical solutions for one-dimensional infiltration problems have been presented in the literature [*Warrick*, 1974; *Srivastava and Yeh*, 1991; *Tracy*, 1995; *Basha*, 1999; among others]. In these solutions, it is assumed that soil properties either are homogeneous or vary deterministically in space. Quantification of uncertainties associated with unsaturated flow in randomly heterogeneous media is challenging. Most relevant studies are numerical, either by Monte Carlo simulations or with numerical moment equation methods [*van Genuchten*, 1982; *Andersson and Shapiro*, 1983; *Yeh et al.*, 1985; *Hopmans et al.*, 1988; *Unlu et al.*, 1990; *Romano et al.*, 1998; *Zhang and Winter*, 1998; *Ferrante and Yeh*, 1999; *Foussereau et al.*, 2000; *Lu et al.*, 2002; *Lu and Zhang*, 2002]. Only a limited number of analytical solutions to the stochastic unsaturated flow problem are available in the literature. These solutions in general are restricted to single-layered, statistically homogeneous porous media. *Yeh et al.* [1985] used spectral representations of heterogeneous soil properties to derive solutions of pressure head statistics for unsaturated flow in the gravity-dominated regime. *Zhang et al.* [1998] gave analytical solutions to the pressure head variance for gravity-dominated flow with both Gardner-Russo and Brooks-Corey constitutive models. *Indelman et al.* [1993] derived expressions for pressure head moments for one-dimensional steady state unsaturated flow in bounded single-layered heterogeneous formations under deterministic boundary conditions (a constant head at the bottom and constant flux at the top). These expressions contain integrals that have to be evaluated numerically in general.

Because of nonlinearity of unsaturated flow, the Kirchhoff transformation is often employed to linearize the equation of unsaturated flow. *Tartakovsky et al.* [1999], using the

Kirchhoff transformation, solved the mean pressure head and the head variance for the one-dimensional unsaturated flow problem up to second order in terms of variability of the log saturated hydraulic conductivity. Although their equations are given in a more general form, the analytical solution for the one-dimensional problem is restricted to a special case of a single-layered soil column with a deterministic pore size distribution parameter under deterministic boundary conditions. *Tartakovsky et al.* [2004] gave an analytical solution to the moments of the Kirchhoff-transformed variable for transient unsaturated flow in statistically homogeneous porous media with an assumption of a deterministic pore-size distribution parameter. Recently, using the Kirchhoff transformation, *Lu and Zhang* [2004] derived analytical solutions to the first two moments (mean and variance) of the pressure head for one-dimensional steady-state unsaturated flow in layered, randomly heterogeneous soils.

In this paper, we first present analytical solutions for the statistics (mean and variance) of the pressure head and the unsaturated hydraulic conductivity for one-dimensional steady state unsaturated flow in a single-layered heterogeneous soil column with random boundary conditions under the assumptions that the constitutive relationship between the pressure head and the unsaturated hydraulic conductivity follows the Gardner model and that the pore size distribution parameter α is a random constant in the layer. The solutions are valid for the entire unsaturated soil column. Specification of random boundary conditions allows us to easily extend the solutions to problems with multiple layers, where the statistics of soil properties in each of these layers may be different. Our solutions are verified using high resolution Monte Carlo simulations. One advantage of the solutions given in this study over those solutions based on the Kirchhoff transformation [*Lu and Zhang*, 2004; *Tartakovsky* *et al.*, 2004] is that the pressure head variance is given explicitly as a function of input variabilities rather than a function of (cross-) covariances of the intermediate Kirchhoff-transformed variables. Such explicit expressions provide more physically meaningful insights.

2 Mathematical Formulation

We start from the equation for steady state flow in a one-dimensional unsaturated single-layered heterogeneous soil column $a \leq z \leq b$,

$$\frac{d}{dz}\left[K(z,\psi)\left(\frac{d\psi}{dz}+1\right)\right]=0, \tag{1}$$

with a constant pressure head at the lower boundary $z = a$,

$$\psi(a) = \Psi_a, \tag{2}$$

and a constant flux boundary at the upper boundary $z = b$,

$$K(z,\psi)\left(\frac{d\psi}{dz}+1\right)\bigg|_{z=b} = -q, \tag{3}$$

where ψ is the pressure head, Ψ_a is the specified pressure head at the bottom of the layer, $K(z,\psi)$ is the unsaturated hydraulic conductivity that depends on the pressure head, q is the flux specified at the top of the layer, and z is the vertical coordinate pointing upwards. Using this coordinate system, the flux q is negative for infiltration and positive for evaporation. Here we assume that both Ψ_a and q are specified with some uncertainties, i.e., $\Psi_a = \langle\Psi_a\rangle + \Psi'$ and $q = \langle q\rangle + q'$, where $\langle\Psi_a\rangle$ and $\langle q\rangle$ are their respective means, and Ψ'_a and q' are their fluctuations. Integrating (1) and using boundary condition (3) yields

$$K(z,\psi)\left(\frac{d\psi}{dz}+1\right) = -q. \tag{4}$$

To solve the above equation, it is required to specify a constitutive relationship between the pressure head and the unsaturated hydraulic conductivity. Although the von Genuchten constitutive model is more accurate and widely used in deterministic simulations, for mathematical convenience we adopt Gardner's exponential model [*Gardner*, 1985]: $K(z,\psi) = K_s(z)\exp[\alpha\psi(z))]$, where $K_s(z)$ is the saturated hydraulic conductivity and α is the pore size distribution parameter. We further assume that K_s is a statistically homogeneous random field, and α is a random constant. The assumption of a random constant α is justified if the ratio of the correlation length of α to the thickness of the layer is relatively large [*Tartakovsky et al.*, 2003; *Lu and Zhang*, 2004]. In the limit that this ratio goes to infinity, the random constant treatment becomes exact.

We formally decompose each random function as a summation of a mean and a fluctuating part: $f(z) = \ln[K_s(z)] = \langle f\rangle + f'(z)$ and $\beta = \ln[\alpha] = \langle\beta\rangle + \beta'$. The log unsaturated hydraulic conductivity then can be written as

$$Y(z) = \ln[K(z)] = \langle f\rangle + f'(z) + \alpha\psi(z) = Y^{(0)}(z) + Y^{(1)}(z) + \cdots, \tag{5}$$

where

$$Y^{(0)}(z) = \langle f\rangle + \alpha_g\psi^{(0)}(z), \tag{6}$$

and

$$Y^{(1)}(z) = f'(z) + \alpha_g\psi^{(1)}(z) + \alpha_g\psi^{(0)}(z)\beta', \tag{7}$$

where $\alpha_g = \exp(\langle\beta\rangle)$ is the geometric mean of α. Because the variability of the pressure head ψ depends on input variabilities, i.e., those of the soil properties (K_s and α) and those of the boundary conditions (Ψ_a and q), one may express ψ as an infinite series in the following form: $\psi(z) = \psi^{(0)} + \psi^{(1)} + \psi^{(2)} + \cdots$, where the order of each term in the series is with respect to σ, which is a combination of standard derivations of the input variables. By substituting (6)-(7) and the decompositions of Ψ_a and q into (4) and (2), and separating terms at different orders up to first order, we have the zeroth-order equation

$$K_m(z,\psi)\left(\frac{d\psi^{(0)}(z)}{dz} + 1\right) = -\langle q\rangle, \tag{8}$$

subject to a boundary condition

$$\psi^{(0)}(a) = \langle \Psi_a \rangle, \tag{9}$$

where $K_m(z) = K_g \exp[\alpha_g \psi^{(0)}(z)]$ is the zeroth-order unsaturated hydraulic conductivity, and K_g is the geometric mean of the saturated hydraulic conductivity. The first-order equation is

$$K_m(z,\psi)\left[\frac{d\psi^{(1)}(z)}{dz} + Y^{(1)}(z)\left(\frac{d\psi^{(0)}(z)}{dz} + 1\right)\right] = -q', \tag{10}$$

subject to a boundary condition

$$\psi^{(1)}(a) = \Psi'_a. \tag{11}$$

2.1 Zeroth-order Mean Pressure Head

By noticing that $K_m(z) = K_g \exp[\alpha_g \psi^{(0)}(z)]$, (8) can be written as

$$\frac{dK_m(z)}{dz} + \alpha_g K_m(z) = -\alpha_g \langle q\rangle, \tag{12}$$

subject to a boundary condition $K_m(a) = K_g \exp[\alpha_g \langle \Psi_a \rangle]$. This equation can be solved directly and the solution is

$$K_m(z) = K_g e^{\alpha_g (a + \langle \Psi_a \rangle - z)} - \langle q\rangle \left(1 - e^{\alpha_g (a-z)}\right). \tag{13}$$

The zeroth-order pressure head $\psi^{(0)}$ can be simply derived from (13):

$$\psi^{(0)}(z) = \frac{1}{\alpha_g} \ln \left[e^{\alpha_g (a + \langle \Psi_a \rangle - z)} - \frac{\langle q \rangle}{K_g} \left(1 - e^{\alpha_g (a-z)} \right) \right]. \tag{14}$$

Similar to *Yeh* [1989], the solution of the mean head for a multiple layered soil column is straightforward. The zeroth-order mean pressure head is solved sequentially from the bottom layer to the top layer. The mean head value computed at the top of a layer is taken as a constant head boundary at the bottom of the overlying layer.

2.2 Variance of Pressure Head

Substituting (8) into (10) yields

$$K_m(z) \frac{d\psi^{(1)}(z)}{dz} - \langle q \rangle Y^{(1)}(z) = -q'. \tag{15}$$

Since $Y^{(1)}(z) = f'(z) + \alpha_g \psi^{(1)}(z) + \psi^{(0)}(z)\beta'$, (15) becomes

$$\frac{d\psi^{(1)}(z)}{dz} - \frac{\alpha_g \langle q \rangle}{K_m(z)} \psi^{(1)}(z) = \frac{-q' + \langle q \rangle f'(z) + \alpha_g \langle q \rangle \psi^{(0)}(z)\beta'}{K_m(z)}. \tag{16}$$

The solution of the above first-order ordinary differential equation with boundary condition (11) is

$$\psi^{(1)}(z) = \frac{e^{\alpha_g (a-z)}}{K_m(z)} \left[K_g e^{\alpha_g \langle \Psi_a \rangle} \Psi'_a + \int_a^z \left[-q' + \langle q \rangle f'(z) + \alpha_g \langle q \rangle \psi^{(0)}(z) \beta' \right] e^{-\alpha_g (a-z)} dz \right], \tag{17}$$

which can be used to formulate the pressure head variance and cross-covariance between the pressure head and other variables.

2.2.1 Single-layer Soil Column

For an unsaturated soil system with a single layer, we may assume that the boundary conditions q and Ψ_a are independent of medium properties f and α. The latter assumption, the independence of Ψ_a on soil properties of the layer, will be justified later. If we further assume that f and α are uncorrelated and α is a random constant, then up to second order, the pressure head covariance $C_\psi(y,z)$ can be derived from (17) as

$$\begin{aligned} C_\psi(y,z) &= \langle \psi^{(1)}(y)\psi^{(1)}(z)\rangle \\ &= \frac{e^{\alpha_g(2a-y-z)}}{K_m(y)K_m(z)}\Big[K_g^2 e^{2\alpha_g\langle\Psi_a\rangle}\sigma^2_{\Psi_a} \\ &+ \int_a^y\int_a^z \left[\sigma_q^2 + \langle q\rangle^2 C_f(y,z) + \alpha_g^2\langle q\rangle^2\psi^{(0)}(y)\psi^{(0)}(z)\sigma_\beta^2\right] e^{-\alpha_g(2a-y-z)}dydz\Big], \end{aligned} \tag{18}$$

where the first term is the contribution of the uncertain boundary condition at the lower boundary to the head covariance at elevations z and y.

Because of symmetry of $C_\psi(y,z)$ with respect to its arguments y and z, we only need to find the solution for $y \geq z$. Integration of the first term in (18) under the double integral is trivial. For an exponential covariance function $C_f(y,z) = \sigma_f^2\exp(-|y-z|/\lambda)$, where λ is the correlation length of f, the integration of the second and third terms can be done analytically and (18) becomes

$$\begin{aligned} C_\psi(y,z) &= \frac{e^{\alpha_g(2a-y-z)}}{K_m(y)K_m(z)}\left\{K_g^2\, e^{2\alpha_g\langle\Psi_a\rangle}\sigma^2_{\Psi_a} + \frac{\sigma_q^2}{\alpha_g^2}(e^{-\alpha_g(a-y)}-1)(e^{-\alpha_g(a-z)}-1)\right. \\ &+ \frac{\langle q\rangle^2\sigma_f^2\lambda^2}{\alpha_g^2\lambda^2-1}\left[\left(1-e^{(\alpha_g-\frac{1}{\lambda})(z-a)} - e^{(\alpha_g-\frac{1}{\lambda})(y-a)} + e^{(\alpha_g+\frac{1}{\lambda})(z-a)+(\alpha_g-\frac{1}{\lambda})(y-a)}\right)\right. \\ &- \left.\left.\frac{e^{2\alpha_g(z-a)}-1}{\alpha_g\lambda}\right] + K_g^2\sigma_\beta^2 F(y)F(z)\right\}, \end{aligned} \tag{19}$$

where

$$F(z) = \psi^{(0)}(z)e^{\alpha_g[z+\psi^{(0)}(z)-a]} + \left(e^{\alpha_g\langle\Psi_a\rangle} + \frac{\langle q\rangle}{K_g}\right)(z-a) - \langle\Psi_a\rangle e^{\alpha_g\langle\Psi_a\rangle}. \tag{20}$$

Equation (19) leads to the expression for the pressure head variance

$$\sigma_\psi^2(z) = \sigma^2_{\Psi_a}e^{2\alpha_g[h_a-\psi^{(0)}(z)-z]} + \frac{\sigma_q^2}{\alpha_g^2K_m^2(z)}\left[e^{\alpha_g(a-z)}-1\right]^2$$

$$
\begin{aligned}
&+ \quad \frac{\langle q\rangle^2\sigma_f^2\lambda^2}{K_m^2(z)(\alpha_g^2\lambda^2-1)}\left[1-2e^{(\alpha_g+\frac{1}{\lambda})(a-z)}+e^{2\alpha_g(a-z)}-\frac{1-e^{2\alpha_g(a-z)}}{\alpha_g\lambda}\right] \\
&+ \quad \sigma_\beta^2\left[\psi^{(0)}(z)+\frac{\langle q\rangle}{K_g}e^{\alpha_g[a-\psi^{(0)}(z)-z]}(z-a)-(h_a-z)e^{\alpha_g[h_a-\psi^{(0)}(z)-z]}\right]^2, \qquad (21)
\end{aligned}
$$

where $h_a = a + \langle\Psi_a\rangle$ is the total head at the lower boundary $z = a$. The first term in the right side of (21) is the contribution of uncertainty due to the variability of the constant head specified at the lower boundary to the head variance at elevation z. As z increases, this contribution decreases, as expected. The second term in the right-hand side represents the effect of uncertainty on the specified flux at the upper boundary. This term has a minimum at the low boundary, increases with elevation z, and reaches its maximum at the top boundary. The last term in (21) is the contribution of variability of α to the head variance. The third group of terms, i.e., the second line of (21), is the contribution of the variability of the saturated hydraulic conductivity to the head variance. In case of $\alpha_g \equiv 1/\lambda$, the denominator of this term is zero and this term can be re-derived by taking its limit as $\alpha_g \to 1/\lambda$:

$$
\sigma_{\psi,f}^2 = \frac{\langle q\rangle^2\lambda^2\sigma_f^2}{2K_m^2(z)}\left\{1+[2\alpha_g(a-z)-1]e^{2\alpha_g(a-z)}\right\}. \qquad (22)
$$

Sometimes, we may be interested only in the behavior of predictive uncertainty of the pressure head within the upper portion (gravity-dominated) of the unsaturated zone. For large z, (21) can be approximated as

$$
\sigma_\psi^2 = \frac{\sigma_q^2}{\alpha_g^2\langle q\rangle^2}+\frac{\lambda\,\sigma_f^2}{\alpha_g(1+\alpha_g\lambda)}+\sigma_\beta^2[\Psi^{(0)}]^2, \qquad (23)
$$

where $\Psi^{(0)}$ is the zeroth-order mean pressure head in the gravity-dominated region of the layer. Note that the second term in (23), the contribution of f variability to the head variability, is identical to that of *Yeh* [1985], which was derived for gravity-dominated unsaturated flow under deterministic boundary conditions.

It should be noted that equation (21) may be used to compute the head variance for the one-dimensional saturated flow problem with a random constant head at one end ($z = a$) and a random constant flux at the other end, simply by setting $\alpha_g = 0$ and $\sigma_\beta^2 = 0$ in (21):

$$\sigma_\psi^2(z) = \sigma_{\Psi_a}^2 + \frac{\sigma_q^2}{K_g^2}(z-a)^2 + \frac{2\langle q\rangle^2\sigma_f^2\lambda}{K_g^2}\left[(z-a) + \lambda\left(e^{(a-z)/\lambda} - 1\right)\right]. \tag{24}$$

Here $\sigma_\psi^2(z)$ is the saturated head variance and $\sigma_{\Psi_a}^2$ is the uncertainty of the constant head boundary.

2.2.2 Multi-layer Soil Column

For a one-dimensional soil column with n layers defined by $z_1 < z_2 < \cdots < z_{n+1}$ and given boundary conditions of an infiltration rate q at the top $z = z_{n+1}$ and a constant pressure head Ψ_{z_1} at the bottom $z = z_1$, again, solutions can be derived upward sequentially from the bottom to the top layer. An important observation is that, for one-dimensional flow problems with the given boundary conditions, the head moments in any individual layer are independent of the soil properties of all overlying layers. Because the flux at the top of the bottom layer is the same as that in the top of the soil column, it is obvious that the head moments for the bottom layer can be solved alone without considering soil properties of all overlying layers. As a result, the head variability at the top of the bottom layer is uncorrelated with soil properties of the second layer, i.e., $\langle\beta'\Psi_2'\rangle = \langle\beta'\psi'(z_2)\rangle = 0$ and $\langle f'(z)\Psi_2'\rangle = \langle f'(z)\psi'(z_2)\rangle = 0$ for $z_2 \leq z \leq z_3$, where Ψ_2' is the variability of the pressure head at the bottom of the second layer, simply because $\psi'(z_2)$ is determined from the bottom layer. This argument is valid for the rest of overlying layers. However, since the flux at the top of interface of a layer is the same as that specified at the top of the soil column, for any layer $k \geq 2$, $\langle q'\psi'(z)\rangle \neq 0$ for $z_{k-1} < z \leq z_k$, i.e., $\langle q'\Psi_k'\rangle = \langle q'\psi\prime(z_k)\rangle \neq 0$.

Based on the above reasoning, the pressure head covariance in any overlying layer k of the multiple-layer soil column can be written as

$$\begin{aligned}
C_\psi(y,z) &= \frac{e^{\alpha_g(2z_k-y-z)}}{K_m(y)K_m(z)}\left[K_g^2 e^{2\alpha_g\langle\Psi_k\rangle}\sigma^2_{\Psi_k}\right.\\
&- K_g e^{\alpha_g\langle\Psi_k\rangle}\left[\int_a^y \langle q'\Psi'_k\rangle e^{\alpha_g(z-z_k)}dz + \int_a^z \langle q'\Psi'_k\rangle e^{\alpha_g(z-z_k)}dz\right]\\
&+ \left.\int_a^y\int_a^z \left[\sigma_q^2 + \langle q\rangle^2 C_f(y,z) + \alpha_g^2\langle q\rangle^2\psi^{(0)}(y)\psi^{(0)}(z)\sigma_\beta^2\right] e^{-\alpha_g(2z_k-y-z)}dydz\right] \quad (25)
\end{aligned}$$

where $z_k \le z < y \le z_{k+1}$, and Ψ_k is the constant head boundary at the bottom of the k^{th} layer and is determined from the underlying $(k-1)^{th}$ layer. Comparing to (18), the only difference is that the cross-covariance $\langle q'\Psi'_k\rangle$ may not be zero and should be evaluated for each sequential layer. This cross-covariance can be approximated up to first order by multiplying q' to (17), taking the mean, and carrying out the integral

$$\langle q'\psi^{(1)}(z)\rangle = \frac{e^{\alpha_g(a-z)}}{K_m(z)}\left[\frac{\sigma_q^2}{\alpha_g}\left(1-e^{\alpha_g(z-a)}\right) + K_g e^{\alpha_g\langle\Psi_a\rangle}\langle q'\Psi'_a\rangle\right]. \quad (26)$$

Applying this equation at the top boundary of the $(k-1)^{th}$ layer $z = z_k$ yields

$$\langle q'\Psi'_k\rangle = \langle q'\psi^{(1)}(z_k)\rangle = \frac{e^{\alpha_g(z_{k-1}-z_k)}}{K_m(z_k)}\left[\frac{\sigma_q^2}{\alpha_g}\left(1-e^{\alpha_g(z_k-z_{k-1})}\right) + K_g e^{\alpha_g\langle\psi^{(0)}(z_{k-1})\rangle}\langle q'\Psi'_{k-1}\rangle\right]. \quad (27)$$

Substituting (27) into (25) and setting $y = z$ leads to the pressure head variance in the k^{th} layer:

$$\begin{aligned}
\sigma_\psi^2(z) &= \sigma_\psi^2(z_k)e^{2\alpha_g(h_k-h)} + \frac{\sigma_q^2}{\alpha_g^2K_m^2(z)}\left[e^{\alpha_g(z_k-z)}-1\right]^2\\
&+ \frac{2K_m(z_k)\langle q'\Psi'_k\rangle}{\alpha_g K_m^2(z)}\left[e^{\alpha_g(z_k-z)}-1\right]e^{\alpha_g(z_k-z)}\\
&+ \frac{\langle q\rangle^2\sigma_f^2\lambda^2}{K_m^2(z)(\alpha_g^2\lambda^2-1)}\left[1-2e^{(\alpha_g+\frac{1}{\lambda})(z_k-z)} + e^{2\alpha_g(z_k-z)} - \frac{1-e^{2\alpha_g(z_k-z)}}{\alpha_g\lambda}\right]\\
&+ \sigma_\beta^2\left[\psi^{(0)}(z) + \frac{\langle q\rangle}{K_g}e^{\alpha_g(z_k-h)}(z-z_k) - (h_k-z)e^{\alpha_g(h_k-h)}\right]^2, \quad (28)
\end{aligned}$$

where $z_k < z \leq z_{k+1}$. In (28), h_k and $\sigma_\psi^2(z_k)$ are respectively the total head and the head variance specified at the bottom of the k^{th} layer, both of which are determined from the $(k-1)^{th}$ layer for $k \geq 2$. The parameters K_g, α_g, σ_f^2, λ, and σ_β^2 in (28) refer to soil properties of the k^{th} layer. The index k in these parameters have been omitted for simplicity in mathematical representation. If $\alpha_g = 1/\lambda$ for some layers, the term on the third line of (28) for these layers should be replaced by the expression in (22).

3 Variance of Log Hydraulic Conductivity

Writing $K(z) = K^{(0)}(z) + K^{(1)}(z) + \cdots$ and recalling $K(z) = K_s \exp(\alpha\psi)$ and $\psi(z) = \psi^{(0)}(z) + \psi^{(1)}(z) + \cdots$, we have

$$K^{(0)}(z) + K^{(1)}(z) + \cdots = K_g(1 + f' + \cdots)e^{\alpha_g\psi^{(0)}(z)}\left[1 + \alpha_g\psi^{(1)}(z) + \alpha_g\psi^{(0)}(z)\beta' + \cdots\right]. \quad (29)$$

Separating (29) at different orders leads to

$$K^{(0)}(z) = K_m(z) = K_g e^{\alpha_g\psi^{(0)}(z)}, \quad (30)$$

and the first-order approximation

$$K^{(1)}(z) = K_m(z)Y^{(1)}(z) = K_m(z)\left[f' + \alpha_g\psi^{(1)}(z) + \alpha_g\psi^{(0)}(z)\beta'\right]. \quad (31)$$

The latter allows us to formulate the variance of the unsaturated hydraulic conductivity

$$\begin{aligned}\sigma_K^2(z) &= K_m^2(z)\sigma_Y^2(z) \\ &= K_m^2(z)\left\{\sigma_f^2(z) + 2\alpha_g C_{f\psi}(z) + \alpha_g^2\left[\sigma_\psi^2(z) + 2\psi^{(0)}(z)C_{\beta\psi}(z) + \sigma_\beta^2[\psi^{(0)}(z)]^2\right]\right\}, \quad (32)\end{aligned}$$

where the cross-covariance $C_{f\psi}(z)$ and $C_{\beta\psi}(z)$ can be derived by respectively multiplying $f'(z)$ and β' to (17), taking ensemble means, and carrying out integration:

$$C_{f\psi}(z) = \frac{\langle q\rangle\lambda\sigma_f^2}{(\alpha_g\lambda + 1)K_m(z)}\left[1 - e^{(\alpha_g+1/\lambda)(a-z)}\right], \quad (33)$$

and

$$C_{\beta\psi}(z) = \sigma_\beta^2 \left[\psi^{(0)}(z) + \frac{\langle q \rangle}{K_g} e^{\alpha_g [a - \psi^{(0)}(z) - z]} (z - a) - (h_a - z) e^{\alpha_g [h_a - \psi^{(0)}(z) - z]} \right]. \qquad (34)$$

4 Illustrative Examples

In this section, we demonstrate the accuracy of our first-order analytical solutions of the mean pressure head and the head variance for one-dimensional steady state unsaturated flow in a hypothetical layered soil column, by comparing our results with those from Monte Carlo simulations.

4.1 Base Case

In our base case, denoted by Case 1, we consider a one-dimensional heterogeneous soil column with three layers. The length of the soil column is 20 m and the thickness of these layers (from the bottom to the top layer) is $5m$, $5m$, and $10m$, respectively. The column is uniformly discretized into 400 line segments (one-dimensional elements) of $0.05m$ in length. The origin of the vertical coordinate is set at the bottom of the column. The mean total head is prescribed at the bottom as $\langle H_a \rangle = 0.0\ m$ (i.e., $\langle \Psi_a \rangle = 0.0$, water table) and $\sigma_{H_a}^2 = \sigma_{\Psi_a}^2 \equiv 0$, and the mean infiltration rate at the top boundary is given as $\langle q \rangle = -0.002\ m/day$ with a standard deviation of $\sigma_q = 0.0004\ m/day$, i.e., coefficient of variation $CV_q = 20\%$. Here we choose a relatively small variability of the infiltration rate to ensure that the Monte Carlo simulations, which are conducted to validate the first-order analytical solutions, will converge. The means of the log saturated hydraulic conductivity for three layers are given as $\langle f \rangle = 0.0$, 1.0, and 0.0, respectively, with $CV_{K_s} = 100\%$ ($\sigma_f^2 = 0.693$) for all layers. The correlation length of the log hydraulic conductivity is $\lambda = 1.0\, m$ for all layers. The statistics of the logarithm of the pore size distribution parameter are given as $\langle\beta\rangle = 0.693$, 1.099, and 0.405, respectively, which gives the geometric mean of $\alpha_g = 2.0, 3.0$, and 1.5. The variability of α is given as $CV_\alpha = 10\%$ for all layers.

To evaluate the accuracy of the first-order analytical solutions, we conduct Monte Carlo simulations for comparison purposes. For three layers, we generate three sets of realizations, each of which includes 10,000 one-dimensional unconditional realizations. Each set of these realizations has been tested separately by comparing their sample statistics (the mean, variance, and correlation length) with the specified mean and covariance functions. The comparisons show that the generated random fields reproduce the specified mean and covariance structure well. Realizations of the log hydraulic conductivity fields for the whole column are then composed using three realizations taken from each set of realizations. The log pore-size distribution parameters for the three layers are generated from a random number generator. In the case of uncertain boundary conditions (a random infiltration rate and/or a random constant head at the lower boundary), boundary values are also generated using the random number generator.

The steady state unsaturated flow equation, i.e. equation (1) subject to boundary conditions (2)-(3), is solved using Yeh's algorithm [*Yeh* , 1989], for each realization of the log hydraulic conductivity field and the pore size distribution parameter for the three layers. In the case that the uncertainties in the infiltration rate and/or constant head boundary condition (at the bottom) are involved, randomly generated values of the infiltration rate and constant head will be used. If a solution for pressure head contains any positive values, the realization corresponding to this solution is simply removed. The sample statistics for the flow field, i.e., the mean prediction of head and its associated uncertainty (variance) are then computed from the rest of realizations. These statistics are considered the "true" solutions that are used to compare against the derived analytical solutions of the moment equations.

Figure 1a compares the mean pressure head derived from Monte Carlo simulations (solid curve) and zeroth-order analytical solutions (dashed curve). It is seen from the figure that the zeroth-order analytical solution is very close to that derived from the Monte Carlo simulations. Comparison of the standard deviation of pressure head computed from Monte Carlo simulations and analytical solutions is illustrated in Figure 1b, which again shows that both are similar.

There are several possible sources of errors that could contribute to the discrepancy between the Monte Carlo results and the analytical solutions. First, there are two types of errors associated with Monte Carlo simulation results: numerical and statistical. The former depends on the numerical method and the particular solver used as well as the spatial discretization. The larger the spatial variability, the finer the required spatial discretization. The statistical errors involved in Monte Carlo simulations stem from approximating the stochastic process of interest with a finite number of realizations. To reduce this type of error, one may need to conduct a large number of simulations. The actual number of required simulations depends on the spatial variability of the process. In our examples, the numerical grid used in Monte Carlo simulations is sufficiently fine (20 elements for each correlation length) to reduce the effect of numerical discretizations, and a considerably large number of realizations (10,000) are used to reduce the statistical errors. On the other hand, the analytical solutions are derived under the assumption of small perturbations, which may introduce error. In particular, the mean head is approximated to zeroth order and the head variance is second order in term of σ, which is a combination of input variabilities. It should be noted that head variance $\sigma_\psi^2[z] = \langle[\psi^{(1)}(z)]^2\rangle$ from analytical solutions represents the lowest-order approximation of the head variance. Here we shall mention that, although the variabilities of f and β in each layer are not large, the total variability of either f or β for the whole column is still relatively large because of the contrast between layers [*Lu and Zhang*, 2002].

Figure 2 illustrates the mean and variance of the unsaturated hydraulic conductivity computed from analytical solutions and Monte Carlo simulations for the base case. It is seen that the first-order analytical solutions are in good agreement with Monte Carlo simulations.

4.2 Large Variabilities on Soil Properties

Next we are interested in validation of our solutions at relative large variabilities of f, β, and q. The problem configuration is similar to the base case, except for the parameter variabilities. We first examine the validation of analytical solutions with uncertainty in each individual parameter while treating other parameters deterministically. Monte Carlo simulations are conducted for each individual case. Figure 3 depicts the comparisons of Monte Carlo results and analytical solutions at $\sigma_f^2 = 2.0$ (coefficient of variation $CV_{K_s} =$ 253%). Note that, at such a large degree of variability, the zeroth-order analytical solution of the mean pressure head deviated slightly from the Monte Carlo results (overestimated in term of the absolute value of the mean head), while the head variance from our analytical solution is in good agreement (slightly overestimated) with that of the Monte Carlo results.

Figure 4 compares Monte Carlo results and analytical solutions for a variability of $CV_\alpha = 30\%$. The figure indicates that there is a large discrepancy in the head variance between the two solutions and that the analytical solutions tend to underestimate both the mean head (in absolute values) and the head variance.

By noticing that the analytical solutions overestimate the contribution of f uncertainty to the head variance but underestimate that of β uncertainty to the head variance, we suspect that errors introduced by uncertainties of these two parameters may be partially cancelled out and more accurate results may be obtained. Figure 5 compares the mean head and head variance derived from Monte Carlo simulations and the analytical solutions for relatively large parameter uncertainties: $CV_{K_s} = 200\%, CV_\alpha = 30\%$, and $CV_q = 20\%$. It is seen from the figure that both the mean head and the head variance from the analytical solutions are reasonably close to Monte Carlo results. This significantly extends the possible range of applicability of analytical solutions to flow in layered porous media with a relatively large degree of heterogeneity.

4.3 Uncertain Boundary Flux

To investigate the effect of boundary flux uncertainty on the mean flow field and the head variance, we conduct several numerical experiments with different magnitudes of the coefficient of variation in q, $CV_q = 0\%, 50\%, 100\%$, and 200%, while the variabilities of the log hydraulic conductivity f and the log pore-size distribution parameter β remain the same as in the base case. Because the variation of the infiltration rate does not affect the zeroth-order mean flow field, we are only concerned with the pressure head variance in our discussion. Figure 6 illustrates the effect of the variability of q on the head variance. It is seen from

Figure 6 that after excluding the effect of the variabilities of f and α, the contribution of q variability to the pressure head variance is linearly proportional to the square of CV_q, i.e., linearly proportional to σ_q^2. This can also be seen from equation (28).

4.4 Uncertain Constant Head Boundary

In most practical problems, it is not easy to precisely specify the pressure head at the lower boundary of an unsaturated soil column. Or sometimes, we are not able to specify the exact location of the water table. As a result, a constant head at the lower boundary should be specified with some uncertainty. We are interested in how this uncertainty will affect our prediction of the mean head and its associated uncertainty. Figure 7 shows the profile of the pressure head variance for different magnitudes of uncertainty on the prescribed constant head at the lower boundary: $\sigma_{\psi_a} = 0.0$, 0.1, 0.5, 1.0, and 10.0. An important observation from the figure is that the contribution of the boundary head uncertainty to the pressure head variance decreases with elevation z and this contribution reduces to zero in the gravity-dominated region. The implication from this observation is that, once the flow in the upper portion of a layer reaches the gravity-dominated regime, the uncertainty of the prescribed head at the bottom of the column will not have any effect on the pressure head uncertainty in all overlying layers.

Another way to look at the effect of uncertainty in the constant head boundary at the bottom of the column on the predictive head variance is to specify different values of the head boundary and to see how the changes to the prescribed head will affect the head uncertainty in the column. Figure 8 shows profiles of the mean head (Fig. 8a) and the head variance (Fig. 8b) for different values of Ψ_a. It is seen from the figure that the variation of the constant head specified at the bottom boundary does have an effect on the predictions. However, if the flow in the upper portion of a layer has reached the gravity-dominated regime, the variation in the constant head value does not have any effect on the overlying layers.

4.5 Relative Contribution of Variabilities in K_s, α, and q

We also conducted three numerical simulations to investigate the relative contribution of the variability of f, β, and q to the pressure head variance. In each simulation, we only allow variation in one of these three parameters with a coefficient of variation $CV_f = 50.0\%$, $CV_\alpha = 15\%$, and $CV_q = 50\%$, while all other parameters are the same as in the base case. The results are illustrated in Figure 9, where the dashed curve, dash-dotted curve, and dotted curve represent the pressure head variance due to the variability of α, K_s, and q, respectively. The solid curve in Figure 9 stands for the pressure head variance due to the variabilities of all three parameters.

It is seen that under the condition of mutually independent K_s, α, and q, the contribution of the variability in each parameter to the pressure head variance is additive, namely, the pressure head variance due to the variabilities of all three parameters equals the sum of the three pressure head variances due to the variability of the individual parameter. In addition, it seems that the variability in the pore size distribution α has the largest contribution to the pressure head variance, compared to other parameters with the same magnitude of coefficients of variation. The finding that unsaturated flow is most sensitive to the variability in α is consistent with the earlier observations made by *Zhang et al.* [1998], where only the effects of f and α were studied.

5 Summary and Conclusions

In this study, we derived first-order analytical solutions to the mean pressure head and the head variability as well as the moments of the unsaturated hydraulic conductivity for one-dimensional steady state unsaturated flow in a layered, randomly heterogeneous soil column under random boundary conditions (a prescribed constant head at the bottom and a flux at the top boundary), with the assumption that the constitutive relation between the unsaturated hydraulic conductivity and the pressure head follows Gardner's exponential model. The solutions are not limited to the gravity-dominated flow regime but are valid for the entire unsaturated zone. One of the advantages of the solutions presented in this study over the previous ones [*Lu and Zhang*, 2004] is that the head variance is implicitly expressed as a function of the input variabilities, i.e, those of the log hydraulic conductivity, the pore-size distribution parameter, and boundary conditions. The accuracy of these solutions is verified using Monte Carlo simulations. Numerical examples show that these solutions are valid for relatively large variabilities in soil properties.

In practice, it is hard to specify precisely the constant pressure head and its associated uncertainty at the lower boundary. An important observation from this study is that once the flow reaches a gravity-dominated regime, the actual value of the pressure head and its variability at the lower boundary do not have any effects on the pressure head statistics in all overlying layers.

The analytical solution confirms our previous conclusion that the variability of the pore size distribution parameter α makes more important contribution to the head variability than the variabilities of the log hydraulic conductivity and the infiltration rate.

References

[1] Andersson, J., and A. M. Shapiro, Stochastic analysis of one-dimensional steady state unsaturated flow: A comparison of Monte Carlo and perturbation methods, *Water Resour. Res.*, 19(1), 121-133, 1983.

[2] Brooks, R.H., and A. T. Corey, Hydraulic properties of porous media, *Hydrol. Pap. 3*, Colo. State Univ., Fort Collins, 1964.

[3] Ferrante, M., and J. T-C Yeh, Head and flux variability in heterogeneous unsaturated soils under transient flow conditions, *Water Resour. Res.*, 35(4), 1471-1479, 1999.

[4] Foussereau, X., W. D. Graham, P. S. C. Rao, Stochastic analysis of transient flow in unsaturated heterogeneous soils, *Water Resour. Res.*, 36(4), 891-910, 2000.

[5] Gardner, W.R., Some steady state solutions of unsaturated moisture flow equations with application to evaporation from a water table, *Soil Sci.*, 85, 228-232, 1958.

[6] Hopmans, J. W., H. Schukking, and P. J. J. F. Torfs. Two-dimensional steady-state unsaturated water flow in heterogeneous soils with autocorrelated soil hydraulic properties, *Water Resour. Res.*, 24(12), 2005-2017, 1988.

[7] Indelman, P., D. Or, and Y. Rubin, Stochastic analysis of unsaturated steady state flow through bounded heterogeneous formations, *Water Resour. Res.*, 29, 1141-1148, 1993.

[8] Lu, Z., S. P. Neuman, A. Guadagnini, and T. M. Tartakovsky, Conditional moment analysis of steady state unsaturated flow in bounded randomly heterogeneous porous soils, *Water Resour. Res.*, 38(4), 10.1029/2001WR000278, 2002.

[9] Lu, Z., and D. Zhang, Stochastic analysis of transient flow in heterogeneous, variably saturated porous media: The van Genuchten-Mualem constitute model. *Vadose Zone J.*, 1:137-149, 2002.

[10] Lu, Z., and D. Zhang, Analytical solutions to steady state unsaturated flow in layered, randomly heterogeneous soils via Kirchhoff transformation, *Advances in Water Resour.*, 27, 775-784, 2004.

[11] Lu, Z., and D. Zhang, On stochastic modeling of flow in multimodal heterogeneous formations, *Water Resour. Res.*, 38(10), doi:10.1029/2001WR001026, 2002.

[12] Polmann, D. J., D. McLaughlin, S. Luis, L. W. Gelhar, and R. Ababou, Stochastic modeling of large-scale flow in heterogeneous unsaturated soils, *Water Resour. Res.*, 27, 1447-1458, 1991.

[13] Protopapas, A. L., and R. L. Bras, The one-dimensional approximation for infiltration in heterogeneous soils, *Water Resour. Res.*, 27, 1019-1027, 1991.

[14] Romano, N., B. Brunone, and A. Santini, Numerical analysis of one-dimensional unsaturated flow in layered soils, *Advs. Water Resources*, 21, 315-324, 1998.

[15] Srivastava, R., and J. T-C Yeh, Analytical solutions for one-dimensional, transient infiltration toward the water table in homogeneous and layered soils. *Water Resour. Res.*, 27,753-762, 1991.

[16] Tartakovsky, D. M., S. P. Neuman, and Z. Lu, Conditional Stochastic Averaging of Steady State Unsaturated Flow by Means of Kirchhoff Transformation, *Water Resour. Res.* , 35(3), 731-745, 1999.

[17] Tartakovsky, D. M., Z. Lu, A. Guadagnini, and A. Tartakovsky, Unsaturated flow in heterogeneous soils with spatially distributed uncertain hydraulic parameters, *J. Hydrology*, 275, 182-193, 2003.

[18] Tracy, F. T., 1-D, 2-D, and 3-D analytical solutions of unsaturated flow in groundwater, *J. Hydrol.*, 170, 199-214, 1995.

[19] Unlu, K., D. R. Nielsen, J. W. Biggar, Stochastic analysis of unsaturated flow: One-dimensional Monte Carlo simulations and comparisons with spectral perturbation analysis and field observations, *Water Resour. Res.*, 26(9), 2207-2218, 1990.

[20] van Genuchten, M. Th., A closed-form equation for predicting the hydraulic conductivity of unsaturated soils, *Soil Sci. Soc. Am. J.*, 44, 892-898, 1980.

[21] van Genuchten, M. Th., A comparison of numerical solutions of one-dimensional unsaturated-saturated flow and mass transport equations, *Adv. Water Res.*, 5,47-55, 1982.

[22] Warrick, A. W., Solution to the one-dimensional linear moisture flow equation with water extraction, *Soil Sci. Soc. Am. J.*, 38, 573-576, 1974.

[23] Yeh, T-C, L. W. Gelhar, A. L. Gutjahr, Stochastic analysis of unsaturated flow in heterogeneous soils: 1. Statistically isotropic media, *Water Resour. Res.*, 21, 447-456, 1985.

[24] Yeh, T-C J., One-dimensional steady-state infiltration in heterogeneous soils, *Water Resour. Res.*, 25(10), 2149-2158, 1989.

[25] Zhang, D., and C. L. Winter, Nonstationary stochastic analysis of steady-state flow through variably saturated, heterogeneous media, *Water Resour. Res.*, 34(5), 1091-1100, 1998.

[26] Zhang, D., T. C., Wallstrom, and C. L., Winter, Stochastic analysis of steady-state unsaturated flow in heterogeneous porous media: Comparison of the Brooks-Corey and Gardner-Russo models, *Water REsour. Res.*, 34(6), 1437-1449, 1998.

[27] Zhang, D., and Z. Lu, Stochastic analysis of flow in a heterogeneous unsaturated-saturated system. *Water Resour. Res.*, 38(2), 10.1029/2001WR000515, 2002.

Figure Captions

Figure 1: Comparisons of analytical solutions (dashed curves) and Monte Carlo simulation results (solid curves) for the base case: (a) mean pressure head, and (b) head variance.

Figure 2: Comparisons of analytical solutions and Monte Carlo simulation results: (a) mean unsaturated hydraulic conductivity and (b) variance of unsaturated hydraulic conductivity for the base case.

Figure 3: Comparison of (a) mean pressure head and (b) head variance derived from analytical solutions and Monte Carlo simulation results for the case with a larger variability of K_s, $CV_{K_s} = 253\%$ ($\sigma_f^2 = 2.0$).

Figure 4: Comparison of (a) mean pressure head and (b) head variance derived from analytical solutions and Monte Carlo simulation results for the case with a larger variability of α, $CV_\alpha = 30\%$.

Figure 5: Comparison of (a) mean pressure head and (b) head variance derived from analytical solutions and Monte Carlo simulation results for the case larger variabilities $CV_{K_s} = 253\%$, $CV_\alpha = 30\%$, $CV_q = 30\%$.

Figure 6: The effect of the variability of the infiltration rate q on the pressure head variance.

Figure 7: The effect of the uncertainty of the specified constant head at the lower boundary on the pressure head variance.

Figure 8: The effect of various values of the specified constant head at the lower boundary on the pressure head variance.

Figure 9: Relative contribution of input variabilities on the pressure head variance.

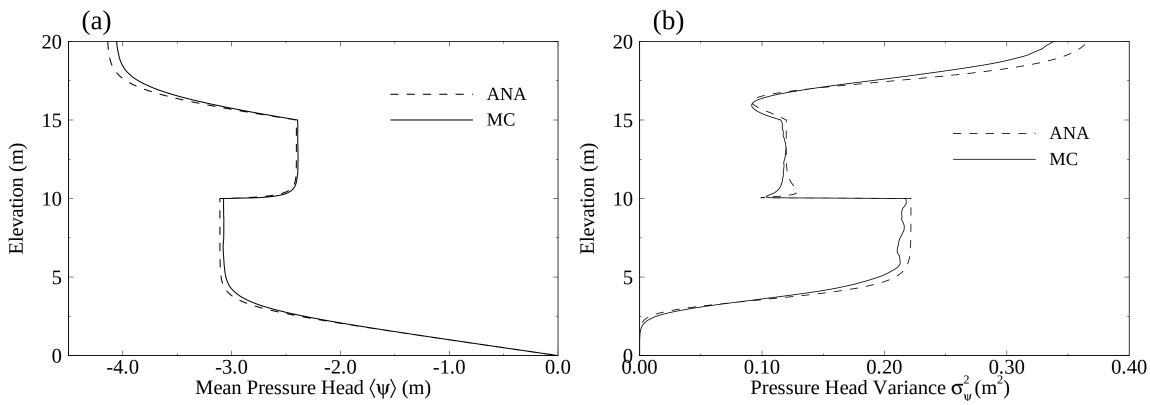

Figure 1:

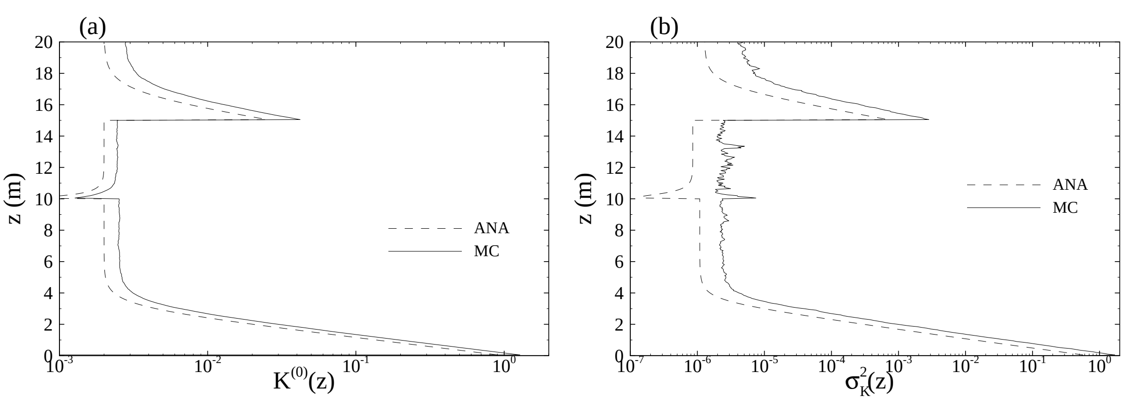

Figure 2:

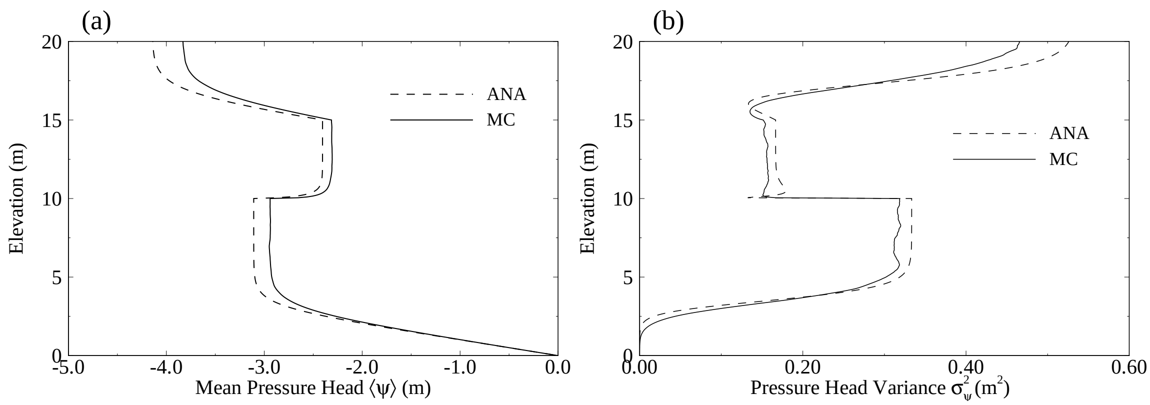

Figure 3:

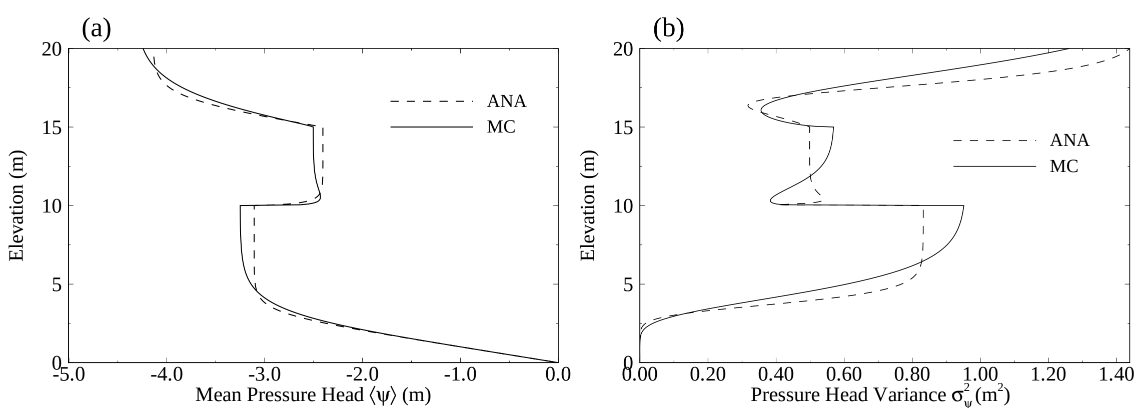

Figure 4:

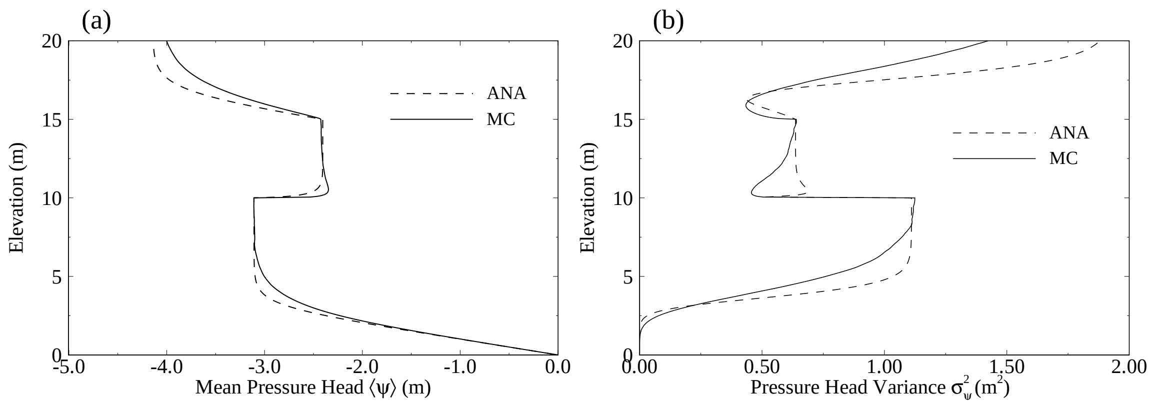

Figure 5:

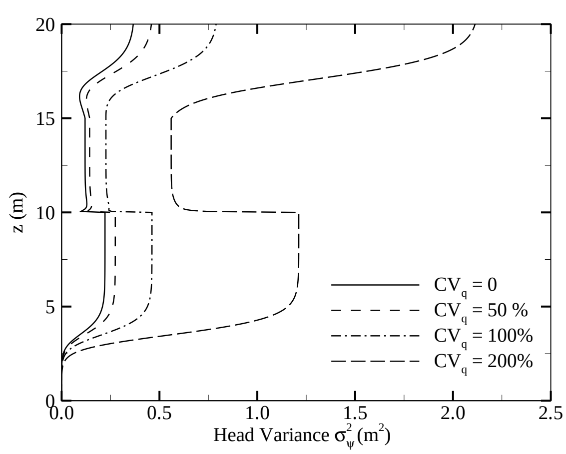

Figure 6:

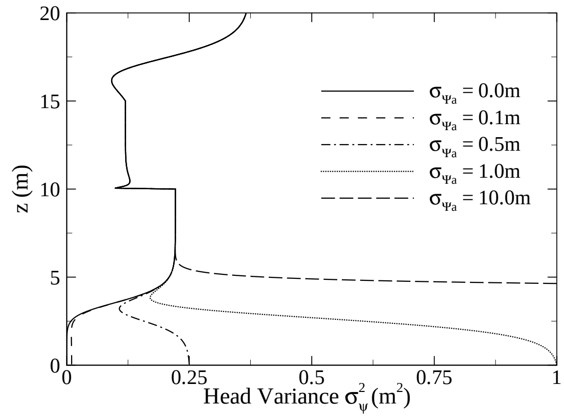

Figure 7:

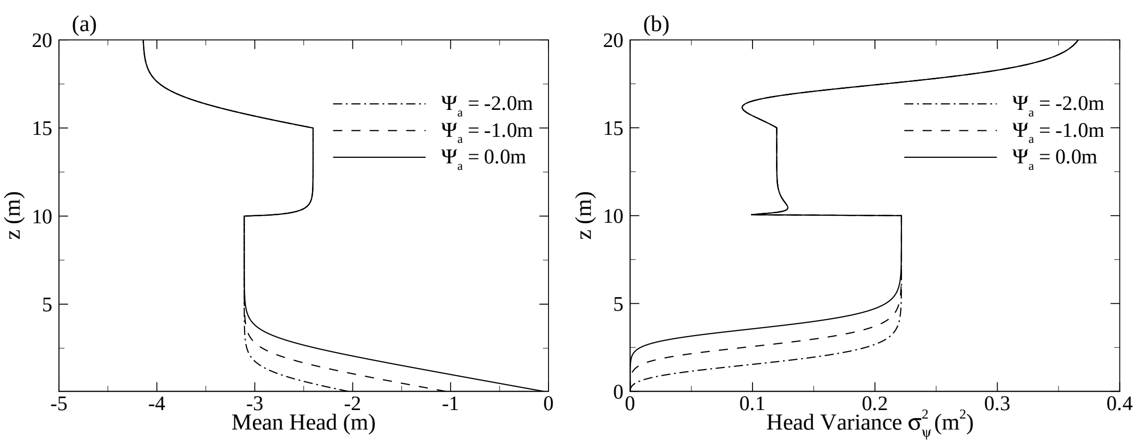

Figure 8:

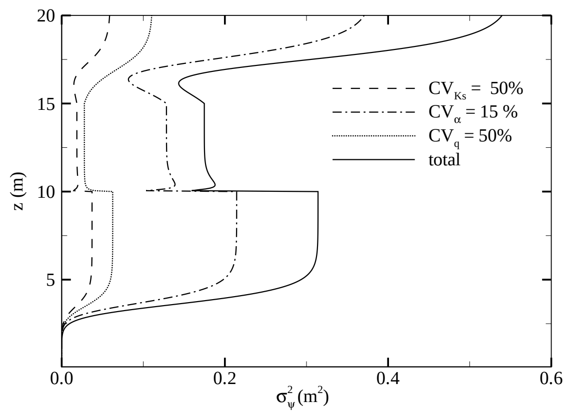

20
15
10
5
z (m)
0.0
0.2
0.4
0.6
$\sigma^2_\psi (m^2)$
CV_{Ks} = 50%
CV_α = 15 %
CV_q = 50%
total

Figure 9: